Inorganic Chemistry

Article

pubs.acs.org/IC

Tetranuclear d-f Metallostars: Synthesis, Relaxometric, and Luminescent Properties

Geert Dehaen,[†] Svetlana V. Eliseeva,[†] Peter Verwilst,[†] Sophie Laurent,[‡] Luce Vander Elst,[‡] Robert N. Muller,[‡,§] Wim De Borggraeve,[†] Koen Binnemans,[†] and Tatjana N. Parac-Vogt*[,†]

[†]Department of Chemistry, KU Leuven - University of Leuven, Celestijnenlaan 200F - P.O. Box 2404, B-3001 Heverlee, Belgium

[‡]NMR and Molecular Imaging Laboratory, Department of General, Organic and Biomedical Chemistry, University of Mons, 7000 Mons, Belgium

[§]Center for Microscopy and Molecular Imaging, 6041 Charleroi, Belgium

Supporting Information

ABSTRACT: A novel ditopic ligand DTPA-ph-phen, based on 1,10-phenanthroline and diethylenetriaminepentaacetic acid (DTPA) units, has been designed and fully characterized by ^{1}H, ^{13}C, and 2D-COSY NMR spectroscopy, IR and electrospray ionization mass spectrometry (ESI-MS) techniques. The DTPA core of the ligand specifically binds Ln(III) ions (Ln = Eu, Gd) resulting in formation of the $[Ln\{DTPA\text{-}ph\text{-}phen\}(H_2O)]^-$ complex. The photophysical properties of the Eu(III) compound have been investigated, and the complex shows characteristic red luminescence with an overall quantum yield of 2.2%. Reaction of $[Gd\{DTPA\text{-}ph\text{-}phen\}(H_2O)]^-$ with Ru(II) leads to further self-assembly into a heterobimetallic metallostar complex containing Gd(III) and Ru(II) in a 3:1 ratio. This tetranuclear $[(Gd\{DTPA\text{-}ph\text{-}phen\})_3(H_2O)_3Ru]^-$ complex (Gd_3Ru), formed by the coordination of Ru(II) to the 1,10-phenanthroline unit, has been characterized by a range of experimental techniques and evaluated toward its feasibility as a potential bimodal optical/MRI agent. The Gd_3Ru metallostar shows intense metal-to-ligand charge transfer (MLCT) transition resulting in intense light absorption in the visible spectral region. Upon irradiation into this MLCT band at 450 nm, the Gd_3Ru complex exhibits red broad-band luminescence in the range of 550−800 nm centered at 610 nm with a quantum yield of 4.8%. Proton nuclear magnetic relaxation dispersion (NMRD) measurements indicate that the Gd_3Ru complex exhibits an enhanced relaxivity value r_1 of 36.0 s^{-1} mM^{-1} per metallostar molecule at 20 MHz and 310 K. The ability of the complex to noncovalently bind to human serum albumin (HSA) was investigated, but no significant interaction was detected.

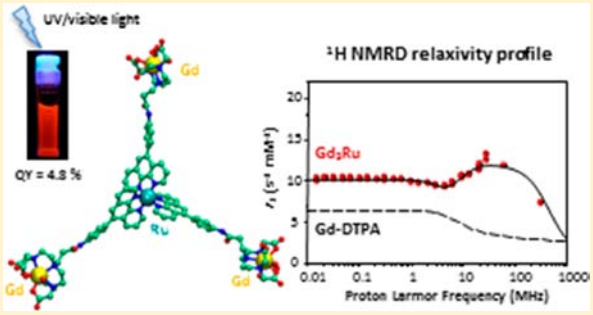

INTRODUCTION

Ever since the introduction of *magnetic resonance imaging* (MRI) as a diagnostic tool, the interest in contrast agents as efficient, responsive and tissue-specific markers has grown tremendously.[1,2] Over the past few years, a change of course has taken place, and the development of multimodal imaging agents has become progressively targeted toward clinical applications.[3−6] Complexes of gadolinium(III) are well-suited T_1-weighted contrast agents because they decrease the relaxation time, T_1, by increasing the relaxation rate of the spins of the surrounding water protons.[7] The effectiveness of this increase is expressed in terms of the *relaxivity*, r_1, which is defined as the increase of the longitudinal relaxation rate in s^{-1} measured in a 1 mM solution of Gd(III). The water proton relaxivity is mainly characterized by four parameters: the number of water molecules in the first coordination sphere of Gd(III) (q), the residence time for these water molecules (τ_M), the relaxation behavior of the electron spin of Gd(III) ($\tau_{S1,2}$), and the rotational diffusion of the complex in solution (τ_R).[8] According to the Solomon−Bloembergen−Morgan theory (SBM-theory), relaxivities up to 100 s^{-1} mM^{-1}could be achieved,[9] and one of the ways to attain higher proton relaxivities is by slowing down the rotational motion of the complex. In the past, several methods have been reported that led to the decrease of the tumbling rate of a Gd(III) complex, for example by incorporating the complex into micelles or liposomes,[10−12] or (non)-covalent binding to a large macromolecule (e.g., protein).[13−15] A more novel approach was described by Desreux and co-workers who reported the formation of a supramolecular structure, also called *metallostar*, containing multiple Gd(III) chelates around a central d-metal ion.[16,17] These supramolecular polymetallic compounds have higher proton relaxivities because of the increase in molecular weight combined with a low degree of internal flexibility.[18,19]

Received: March 12, 2012
Published: July 27, 2012

   dx.doi.org/10.1021/ic300537y | *Inorg. Chem.* 2012, 51, 8775−8783

By combining multiple complementary imaging techniques, the inherent limitations related with one individual technique can be overcome. The development of bimodal imaging agents associating MRI and luminescence-based imaging take advantage of the strengths of both imaging techniques.[5] Whereas MRI is ideal for whole body images because of its good spatial resolution,[20] luminescence-based imaging is able to provide high-resolution images.[21] To date, several complexes containing a fluorescent dye,[6,22−24] transition metal complex,[7,22] or quantum dots[25−28] bound to an MRI or PET agent have been reported. However, the choice of a suitable metal ion is restricted to those showing emission in the red end of the visible spectrum or near-infrared (NIR) so that it provides radiation that can penetrate more easily and effectively into tissues.[22,29] These requirements are successfully fulfilled by the development of Ru(II) complexes because they possess excellent light-harvesting properties combined with long-lived metal-to-ligand charge transfer (MLCT) states and intense luminescence at the red end of the visible spectrum. The Ru(II) ion is a commonly used metal ion because of its exceptional photochemical and photophysical properties[30−34] and frequently reported by Faulkner and co-workers as a sensitizer of near-infrared (NIR) emission of lanthanide ions in f-d heterometallic dyads.[35−38] Although reports dealing with bimodal agents are emerging in the literature, the design of f-d metallostar based imaging agents remain quite scarce. In 2009, Moriggi et al. reported a complex with six Ln(III)-DTTA moieties attached to a single Ru(II) center.[7] The Gd(III)−Ru(II) analogue of such heptametallic species has shown a capability to act as MRI contrast agent, while the Eu(III)−Ru(II) complex displayed interesting luminescent properties.

In our recent study we reported a first example of a Gd(III)/Ti(IV) metallostar complex that has been suggested as a potential MRI/optical bimodal agent.[39] The ditopic DTPA-catechol ligand was able to bind Gd(III) ions and further self-assemble with Ti(IV) resulting into a stable metallostar molecule with 3:1 Gd(III)/Ti(IV) ratio. Although the complex exhibited a high relaxivity of 36.9 s^{-1} mM^{-1} per metallostar molecule at 20 MHz, its optical properties were rather poor as the ligand was not specifically optimized to give highly luminescent complexes. Under UV excitation, the Gd(III)/Ti(IV) metallostar complex exhibited broad-band green emission with a quantum yield of 0.054%. In another study a heterotrimetallic complex Ru_2Gd assembled by the ligand bearing a diethylenetriaminepentaacetic acid (DTPA) moiety and 1,10-phenanthroline was reported.[40] The complex showed bright red luminescence (quantum yield 4.7%) under visible light excitation while a rather moderate relaxivity of 7.0 s^{-1} mM^{-1} per molecule at 20 MHz was obtained. As a next step, in this paper, we describe the synthesis of a new ligand DTPA-ph-phen, bearing a 1,10-phenanthroline and a DTPA-moiety, linked via an amide bond (Scheme 1). In the presence of lanthanide(III) ions, this ligand is able to form stable complexes, $[Ln\{DTPA\text{-}ph\text{-}phen\}(H_2O)]^-$ (Ln = Eu, Gd), and self-assembles further upon addition of Ru(II) into tetranuclear metallostars, $[Ln\{DTPA\text{-}ph\text{-}phen\}_3Ru(H_2O)_3]^-$, with favorable functional properties. Relaxometric and luminescent properties of $[(Gd\{DTPA\text{-}ph\text{-}phen\})_3(H_2O)_3Ru]^-$ have been studied in detail, as well as its ability to bind to Human Serum Albumin (HSA). In addition, the monometallic complex, $[Eu\{DTPA\text{-}ph\text{-}phen\}(H_2O)]^-$ has been synthesized, and its photophysical properties have been investigated to gain information about the coordination environment and solvation numbers of the lanthanide(III) ion.

Scheme 1. Synthesis of DTPA-ph-phen[a]

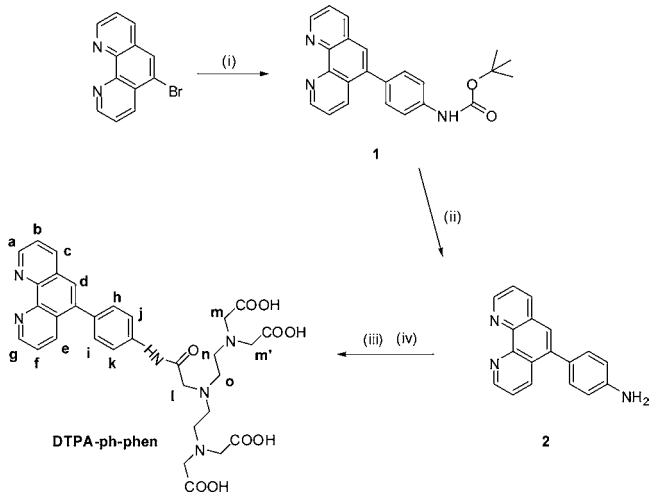

[a]Conditions: (i) *tert*-butyl [4-(4,4,5,5-tetramethyl-1,3,2-dioxaborolan-2-yl)phenyl]carbamate, Cs_2CO_3, $Pd(PPh_3)_4$, reflux, 16 h; (ii) TFA, room temperature, overnight; (iii) DTPA-precursor, TBTU, DIPEA, dry DMF; (iv) HCl 6N.

EXPERIMENTAL SECTION

Synthesis. Reagents were purchased from commercial sources, and used as such without further purification. Dimethylformamide (DMF) was dried overnight over 4A molecular sieves, followed by decantation of the drying agent and vacuum distillation.

Synthesis of 5-Bromo-1,10-phenanthroline. 5-Bromo-1,10-phenanthroline was prepared according to a literature procedure.[41]

Yield: 68%. Mp: 113 °C. ^{1}H NMR (300 MHz, $CDCl_3$, ppm): δ 9.20 (m, 2H), 8.66 (d, 1H, J = 7.8 Hz), 8.17 (dd, J = 1.8 Hz, J = 8.2 Hz, 1H), 8.13 (s, 1H), 7.74 (dd, J = 4,1 Hz, J = 8.3 Hz, 1H), 7.65 (dd, J = 4.5 Hz, J = 8.2 Hz, 1H). ^{13}C NMR (150 MHz, $CDCl_3$, ppm): δ 151.33, 151.10, 147.01, 146.03, 136.35, 135.52, 130.08, 129.20, 128.31, 124.23, 124.07, 121.22. HRMS (EI). Calcd. for $C_{12}H_7BrN_2$ [M]: m/z = 257.9793, found: m/z = 257.9792.

Synthesis of *tert*-Butyl [4-(1,10-phenanthrolin-5-yl)phenyl]-carbamate (1). To a solution of 5-bromo-1,10-phenanthroline (79.8 mg, 0.31 mmol), *tert*-butyl [4-(4,4,5,5-tetramethyl-1,3,2-dioxaborolan-2-yl)phenyl]carbamate (538 mg, 1.69 mmol, 1.1 equiv), and Cs_2CO_3 (1.01 g, 3.10 mmol, 2 equiv) in a 1:1 H_2O/toluene biphasic mixture (32 mL) was added 10 mol % of $Pd(PPh_3)_4$ (178 mg), and the resulting solution was refluxed for 16 h. The reaction mixture was added to CH_2Cl_2 (100 mL) and water (100 mL) and thoroughly stirred, and the organic layer was separated. The aqueous layer was extracted twice with CH_2Cl_2 (100 mL), the combined organic layer was dried over Na_2SO_4 and evaporated in vacuo, and the residue was purified by column chromatography [silica gel, CH_2Cl_2 (saturated NH_3)]. After evaporation, the product was recrystallized from hot toluene (25 mL) and collected as a white solid (387 mg, 68%).

Mp: > 250 °C, product starts to decompose at 258 °C. ^{1}H NMR (300 MHz, $CDCl_3$, ppm): δ 9.20 (s, 2H), 8.30 (dd, J = 1.4 Hz, J = 8.2 Hz, 1H), 8.24 (d, J = 8.3 Hz, 1H), 7.71 (s, 1H), 7.65 (dd, J = 4.5 Hz, J = 8.1 Hz, 1H), 7.60−7.55 (m, 3H), 7.46 (d, J = 8.3 Hz, 2H), 6.71 (s, 1H), 1.56 (s, 9H).^{13}C NMR (150 MHz, $CDCl_3$, ppm): δ 153.19, 150.61, 150.45, 146.85, 146.14, 138.82, 138.73, 136.32, 134.96, 133.82, 130.99, 129.45, 128.63, 126.76, 123.74, 123.19, 119.01, 81.29, 28.75. HRMS (EI). Calcd. for $C_{23}H_{21}N_3O_2$ [M]: m/z = 371.1634, found: m/z = 371.1632.

Synthesis of 4-(1,10-Phenanthrolin-5-yl)aniline (2). To a solution of *tert*-butyl [4-(1,10-phenanthrolin-5-yl)phenyl]carbamate (387 mg, 1.04 mmol) in CH_2Cl_2 (10 mL) was added TFA (10 mL)

dx.doi.org/10.1021/ic300537y | Inorg. Chem. 2012, 51, 8775−8783

dropwise, and the solution was stirred overnight at room temperature. The solvent was removed in vacuo, and the residue was purified by column chromatography [silica gel, CH_2Cl_2 (saturated NH_3)] and collected as a yellow solid (229 mg, 81%).

Mp: > 250 °C, product starts to decompose at 270 °C. ^{1}H NMR (300 MHz, $CDCl_3$, ppm): δ 9.18 (m, 2H), 8.37 (d, J = 8.3 Hz, 1H), 8.21 (d, J = 8.3 Hz, 1H), 7.69 (s, 1H), 7.62 (dd, J = 8.3 Hz, J = 4.6 Hz, 1H), 7.57 (dd, J = 8.3 Hz, J = 4.6 Hz, 1H), 7.32 (d, J = 8.4 Hz, 2H), 6.84 (d, J = 8.4 Hz, 2H), 3.87 (br. s, 2H). ^{13}C NMR (150 MHz, $CDCl_3$, ppm): δ 150.29, 146.89, 146.76, 145.95, 139.40, 136.19, 135.13, 131.35, 129.19, 128.66, 126.39, 123.65, 123.07, 115.41. HRMS (EI). Calcd. for $C_{18}H_{13}N_3$ [M]: m/z = 271.1109, found: m/z = 271.1110.

Synthesis of 1,10-Phenanthroline Derivative (DTPA-ph-phen). To a mixture of *N,N*-bis{*N,N*-bis[(*tert*-butoxycarbonyl)-methyl]-ethylamine}-glycine[35] (41.4 mg, 0.078 mmol, 1 equiv), *o*-benzotriazol-1-yl-*N,N,N′,N′* tetramethyluronium tetrafluoroborate (TBTU) (37.8 mg, 0.118 mmol, 1.5 equiv) and DIPEA (10.1 mg, 0.078 mmol, 1 equiv) in dry DMF (6 mL), was added dropwise a solution of 4-(1,10-phenanthrolin-5-yl)aniline (**2**) (21.2 mg, 0.078 mmol, 1 equiv) dissolved in dry DMF, and the mixture was stirred under argon atmosphere at room temperature overnight. DMF was removed by vacuum evaporation, the crude product was redissolved in dichloromethane and washed with a sodium hydrogen carbonate and saturated sodium chloride solution. The yellow oil was purified by column chromatography [silica gel, CH_2Cl_2 → CH_2Cl_2/MeOH (100/3)]. The obtained yellow oil was immediately redissolved in 5 mL of 6 N HCl. The mixture was stirred at room temperature for 1 h and then washed with dichloromethane (2 times 10 mL). The aqueous solution was concentrated, redissolved in 2 mL of HCl (6N) and the 1,10-phenanthroline derivative, DTPA-ph-phen, precipitated in the course of 2 days as a yellow solid (31.2 mg, 62%).

^{1}H NMR (300 MHz, D_2O, ppm): δ 9.10 (t, 2H), 8.80 (d, 1H), 8.71 (d, 1H), 8.05 (dd, 1H), 8.00 (s, 1H), 7.96 (dd, 1H), 7.56 (d, 2H), 7.45 (d, 2H), 3.97 (s, 8H), 3.63 (s, 2H), 3.50 (t, 4H), 3.13 (t, 4H); ^{13}C NMR (75 MHz, D_2O, ppm): δ 171.29, 170.89, 150.51, 150.39, 146.83, 146.07, 139.12, 138.88, 136.29, 135.04, 134.30, 130.68, 128.55, 128.43, 126,68, 123.71, 123.13, 120.29, 81.52, 59.52, 56.45, 54.28, 52.37, 28.55. ESI-MS. Calcd. for $C_{32}H_{34}N_6O_9$ [M]: m/z = 647.6 ([M+H]$^+$), found: m/z = 647.3 ([M+H]$^+$). IR (KBr): 1730 (CO free acid), 1679 (CO amide) cm^{-1}.

Synthesis of Lanthanide(III) Complexes. The lanthanide(III) complexes of the DTPA-ph-phen ligand were synthesized according to a general procedure: a solution of hydrated $LnCl_3$ salt (1.05 equiv) in H_2O was added to DTPA-ph-phen (1 equiv) dissolved in pyridine, and the mixture was heated at 70 °C for 3 h. The solvents were evaporated under reduced pressure, and the crude product was then refluxed in ethanol for 1 h. After cooling to room temperature, the complex was filtered off and dried in a vacuum. The absence of free lanthanide ions was checked by using an arsenazo indicator solution.

Eu(III) complex [Eu{DTPA-ph-phen}(H_2O)]$^-$. Yield: 75%. IR (KBr, cm^{-1}): 1583 (COO^- asym. stretch), 1517 (amide II), 1396 (COO^- sym. stretch). ESI-MS. Calcd. for $C_{32}H_{30}EuN_6O_9$ [M]: m/z = 818.6 ([M+Na+H]$^+$) and 840.6 ([M+2Na]$^+$), found: m/z = 817.7 ([M+Na+H]$^+$) and 840.7 ([M+2Na]$^+$). HPLC (Solvent A: H_2O + 0.1% HCOOH, Solvent B: ACN, 0% B → 30% B, 35 min): t_r = 20.91 min.

Gd(III) complex [Gd{DTPA-ph-phen}(H_2O)]$^-$. Yield: 78%. IR (KBr, cm^{-1}): 1585 (COO^- asym. stretch), 1518 (amide II), 1398 (COO^- sym. stretch). ESI-MS. Calcd. for $C_{32}H_{30}GdN_6O_9$ [M]: m/z = 845.9 ([M+2Na]$^+$), found: m/z = 845.2 ([M+2Na]$^+$). HPLC (Solvent A: H_2O + 0.1% HCOOH, Solvent B: ACN, 0% B → 30% B, 35 min): t_r = 19.91 min.

Synthesis of Ruthenium(II)−Gadolinium(III) Complex. [Gd{DTPA-ph-phen}(H_2O)]$^-$ (6 mg, 0.0075 mmol, 3 equiv) and hydrated ruthenium tris-chloride (0.46 mg, 0.0023 mmol, 0.9 equiv) were dissolved in an 1:1 ethanol/water mixture (2 mL), and the solution was refluxed overnight under argon atmosphere. The solvent was evaporated to dryness, and the crude product was purified by HPLC to remove remaining starting product. The collected fractions were concentrated under reduced pressure and dried under vacuum at 50 °C overnight.

Ru(II)−Gd(III) complex [(Gd{DTPA-ph-phen})$_3$(H_2O)$_3$Ru]$^-$. Yield: 64%. IR (KBr, cm^{-1}): 1578 (COO^- asym. stretch), 1516 (amide II), 1395 (COO^- sym. stretch). ESI-MS. Calcd. for $C_{96}H_{90}Gd_3N_{18}O_{27}Ru$ [M]: m/z = 358.3 ([M+8H]$^{7+}$) and 367.8 ([M + 3Na +5H]$^{7+}$), found: m/z = 357.2 ([M+8H]$^{7+}$) and 367.7 ([M + 3Na +5H]$^{7+}$). HPLC (Solvent A: H_2O + 0.1% HCOOH, Solvent B: ACN, 0% B → 30% B, 35 min): t_r = 26.66 min. The ratio of Ru/Gd determined by ICP-MS method was 1.00:3.04.

Instruments. ^{1}H and ^{13}C NMR spectra were recorded by using a Bruker Avance 300 spectrometer (Bruker, Karlsruhe, Germany), operating at 300 MHz for ^{1}H and 75 MHz for ^{13}C, or on a Bruker Avance 600 spectrometer, operating at 600 MHz for ^{1}H and 150 MHz for ^{13}C. IR spectra were measured by using a Bruker Alpha-T FT-IR spectrometer (Bruker, Ettlingen, Germany), and data were processed with OPUS 6.5 software. The LC/MS data were collected using an Agilent 1100 system coupled to an Agilent 6110 single-quadrupole MS system. The LC/MS method used a Grace Prevail RP-C18 column (150 mm ×2.1 mm; particle size 3 μm). Samples for ESI-MS were prepared by dissolving the product (2 mg) in methanol (1 mL), then adding 200 μL of this solution to a water/methanol mixture (50:50, 800 μL). The resulting solution was injected at a flow rate of 5 μLmin^{-1}. Mass spectra were obtained by using a Thermo Finnigan LCQ Advantage mass spectrometer. Preparative HPLC was performed using a Waters Delta 600 system equipped with a Waters 996 photodiode-array detector. The preparative HPLC method used a Phenomenex Luna C18 column (150 mm ×21.20 mm; particle size 5 μm). Melting points were determined using a Reichert-Jung Thermovar apparatus and were uncorrected.

Photophysical Measurements. Absorption spectra were measured on a Varian Cary 5000 spectrophotometer on freshly prepared aqueous solutions in quartz Suprasil cells (115F-QS) with an optical path-length of 0.2 cm. Emission data were recorded on Edinburgh Instruments FS920 steady state spectrofluorimeter. This instrument is equipped with a 450W xenon arc lamp, a microsecond flashlamp μF900H (60W) and an extended red-sensitive photomultiplier (185−1010 nm, Hamamatsu R 2658P). All spectra are corrected for the instrumental functions. Luminescence lifetimes of the $^5D_0$ level for Eu(III)-containing solutions were measured on an Edinburgh Instruments FS920 steadystate spectrofluorimeter under 280−310 nm excitation. Lifetimes are averages of at least three independent measurements. Quantum yields were determined by a comparative method using Rhodamine 101 (Aldrich) in ethanol (Q = 100%) as a standard.[42]

Model. The model was built using the Avogadro software.[43] The central part containing the Ru(II) ion and the three 1,10-phenanthroline molecules and the arms including Gd(III) were optimized separately with the Universal Force Field (UFF).[44]

Proton NMRD. Proton nuclear magnetic relaxation dispersion (NMRD) profiles were measured on a Stelar Spinmaster FFC, fast field cycling NMR relaxometer (Stelar, Mede (PV), Italy) over a magnetic field strength range extending from 0.24 mT to 0.7 T. Measurements were performed on 0.6 mL samples contained in 10 mm o.d. pyrex tubes. Additional relaxation rates at 20, 60, and 300 MHz were respectively obtained on a Minispec mq20, a Minispec mq60, and a Bruker AVANCE-300 spectrometer (Bruker, Karlsruhe, Germany). The proton NMRD curves were fitted using data-processing software,[45] including different theoretical models describing the nuclear relaxation phenomena (Minuit, CERN Library).[46−48]

Viscosity. The viscosity was measured at 37 °C using a Cannon-Fenske viscosimeter (ASTM D 445)

RESULTS AND DISCUSSION

Ligand and Complexes. Suzuki cross-coupling of 5-bromo-1,10-phenanthroline with *tert*-butyl [4-(4,4,5,5-tetramethyl-1,3,2-dioxaborolan-2-yl)phenyl]carbamate in the presence of Cs_2CO_3 and $Pd(PPh_3)_4$ in a water/toluene mixture (1:1, v/v) yielded the Boc-protected aniline (**1**), which upon

dx.doi.org/10.1021/ic300537y | Inorg. Chem. 2012, 51, 8775−8783

deprotection by trifluoroacetic acid (TFA) gave compound (**2**). The 1,10-phenanthroline-DTPA based ligand, DTPA-ph-phen, was prepared by coupling 4-(1,10-phenanthrolin-5-yl)aniline (**2**) with the DTPA derivative *N,N*-bis{*N,N*-bis[(*tert*-butoxycarbonyl)methyl]-ethylamine}-glycine,[39] of which only the central carboxylic group remained unprotected, in the presence of *o*-benzotriazol-1-yl-*N,N,N′,N′* tetramethyluronium tetrafluoroborate (TBTU) and DIPEA in dry DMF.

The amide bond between both entities will ensure a high stability of the ligand in vivo. After deprotection of the *tert*-butyl groups, DTPA-ph-phen was obtained as a yellow solid (Scheme 1). A proton NMR spectrum of ligand DTPA-ph-phen was recorded in D_2O of which the peaks correspond to the labeled molecule in Scheme 1 (see the Supporting Information, Figure S1). Further, DTPA-ph-phen was also characterized by 2D COSY spectrum (See the Supporting Information, Figure S2). The ESI-MS spectrum of ligand DTPA-ph-phen in the positive mode showed the molecular ion peak corresponding to $[M+H]^+$ at respectively m/z = 647.3. Lanthanide(III) complexes $[Ln\{DTPA\text{-}ph\text{-}phen\}(H_2O)]^-$ were obtained by reacting ligand DTPA-ph-phen with the corresponding Ln(III) chloride (Ln = Eu, Gd) in pyridine solution. All complexes were purified by Chelex 100 to remove free lanthanide ions from the reaction mixture, and their purity was checked with an arsenazo indicator solution.[49] Positive mode ESI-MS showed molecular peaks $[M+Na+H]^+$ and $[M+2Na]^+$ at respectively m/z = 817.7 and 840.7 corresponding to the Eu(III) complex. The molecular peak $[M+2Na]^+$ at m/z = 845.2, corresponding to the Gd(III) complex, was also detected.

To obtain a metallostar complex, $[Gd\{DTPA\text{-}ph\text{-}phen\}(H_2O)]^-$ was reacted with hydrated ruthenium(III) chloride in an ethanol/water mixture (1:1, v/v) (Scheme 2). The color of the solution changed from colorless to dark orange when the Ru(III) ion is reduced to Ru(II). The Ru(II)−Gd(III) complex was purified by semipreparative reversed-phase HPLC and ESI-MS and HPLC indicated the formation of a 3:1 metallostar compound showing molecular peaks $[M+8H]^{7+}$ and $[M+3Na+5H]^{7+}$ at m/z = 357.2 and 367.7, respectively. Hence, we can represent the structure of the final compound as $[(Gd\{DTPA\text{-}ph\text{-}phen\})_3(H_2O)_3Ru]^-$ or (Gd_3Ru) as shown in Figure 1.

Photophysical Properties. Ru(II)-Centered Absorption and Luminescence. The electronic absorption spectra of ligand DTPA-ph-phen (ε = 84 633 M^{-1} cm^{-1}), $[Gd\{DTPA\text{-}ph\text{-}phen\}(H_2O)]^-$ (ε = 78 599 M^{-1} cm^{-1}) and $[(Gd\{DTPA\text{-}ph\text{-}phen\})_3\ Ru(H_2O)_3]^-$ (ε = 317 553 M^{-1} cm^{-1}) show an intense ligand-centered band at 257 nm (see Supporting Information, Figure S3). The shoulder at 310 nm (ε = 93 974 M^{-1} cm^{-1}) can be attributed to $\pi\rightarrow\pi^*$ and/or to Ru(II)-centered d→d transitions. In addition, $[(Gd\{DTPA\text{-}ph\text{-}phen\})_3(H_2O)_3Ru]^-$ presents a broad band due to spin-allowed d→π^* metal-to-ligand charge transfer (^{1}MLCT) transitions with maxima at 453 nm (ε = 28 963 M^{-1} cm^{-1}) and 422 nm (ε = 28 537 M^{-1} cm^{-1}) (Supporting Information, Figure S3 and Figure 2, left). The excitation spectrum of $[(Gd\{DTPA\text{-}ph\text{-}phen\})_3(H_2O)_3Ru]^-$ recorded by monitoring emission at 610 nm resembles the absorption spectrum (Figure 2, left). Upon excitation into the ^{1}MLCT band at 450 nm, $[(Gd\{DTPA\text{-}ph\text{-}phen\})_3(H_2O)_3Ru]^-$ exhibits red broad-band luminescence centered at 610 nm which is originating from the ^{3}MLCT excited states (Figure 2, right). The quantum yield of $[(Gd\{DTPA\text{-}ph\text{-}phen\})_3(H_2O)_3Ru]^-$ was detemined with Rhodamine 101 as a standard and equals 4.8(4) %. In general,

Scheme 2. Formation of the $[(Gd\{DTPA\text{-}ph\text{-}phen\})_3(H_2O)_3Ru]^-$ Complex[a]

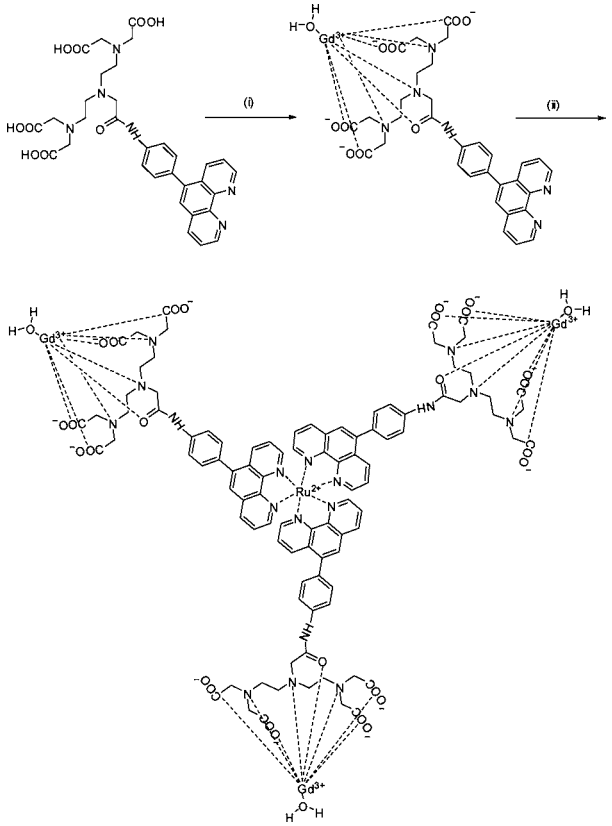

[a](i) $GdCl_3{\cdot}6H_2O$, pyridine; (ii) $RuCl_3{\cdot}xH_2O$, ethanol/water (1:1, v/v).

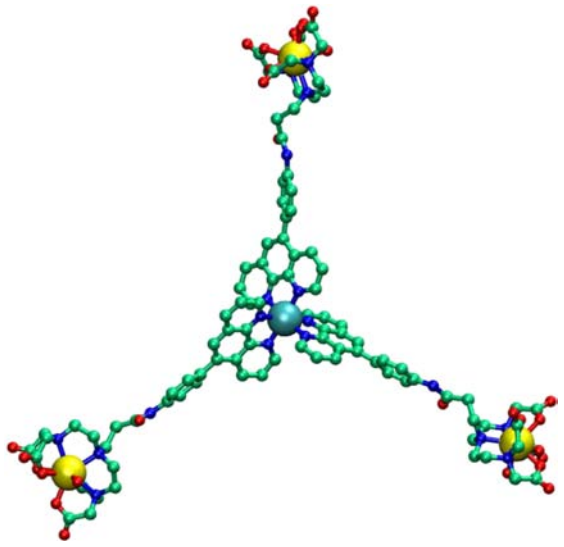

Figure 1. Framework molecular model of the $[(Gd\{DTPA\text{-}ph\text{-}phen\})_3(H_2O)_3Ru]^-$complex. Hydrogen atoms have been omitted for clarity.

the photophysical parameters of $[(Gd\{DTPA\text{-}ph\text{-}phen\})_3(H_2O)_3Ru]^-$ are comparable with those of other luminescent Ru(II) complexes.[29,30]

Eu(III)-Centered Luminescence. To gain more information about the coordination environment around the lanthanide ion, the photophysical properties of [Eu{DTPA-ph-phen}-

dx.doi.org/10.1021/ic300537y | Inorg. Chem. 2012, 51, 8775−8783

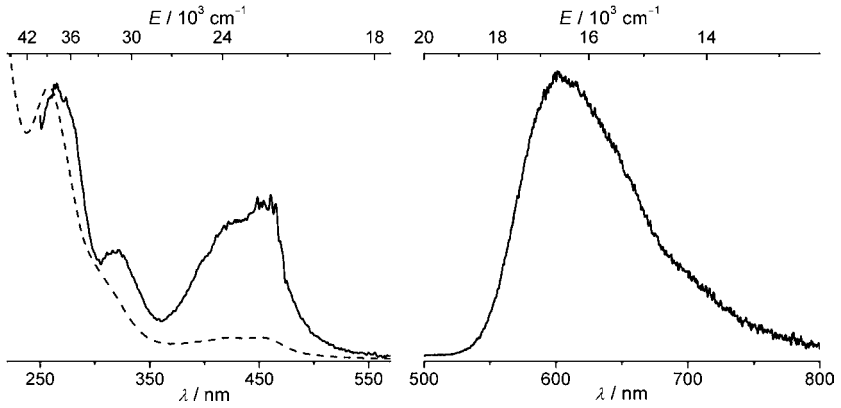

Figure 2. (Left) Excitation (full line, λ_{em} = 610 nm) with superimposed absorption (dashed line) and (right) emission (λ_{ex} = 450 nm) spectra of $[(Gd\{DTPA\text{-}ph\text{-}phen\})_3(H_2O)_3Ru]^-$ in water at room temperature.

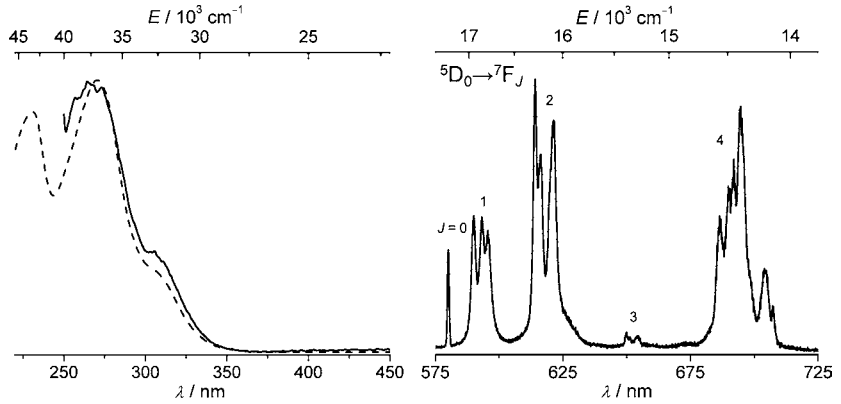

Figure 3. (Left) Excitation (full line, λ_{em} = 614 nm) with superimposed absorption (dashed line) and (right) emission (λ_{ex} = 310 nm) spectra of $[Eu\{DTPA\text{-}ph\text{-}phen\}(H_2O)]^-$ in water at room temperature.

$(H_2O)]^-$ in water solution have been investigated. The excitation spectrum of $[Eu\{DTPA\text{-}ph\text{-}phen\}(H_2O)]^-$, recorded by monitoring the emission at 614 nm, resembles the absorption spectrum and exhibits a broad ligand-centered band with a maximum at ~270 nm and a shoulder at ~310 nm (Figure 3, left). Upon UV excitation, $[Eu\{DTPA\text{-}ph\text{-}phen\}(H_2O)]^-$ displays characteristic red emission due to $^5D_0 \rightarrow {}^7F_J$ (J = 0–4) transitions (Figure 3, right). The hypersensitive transition $^5D_0 \rightarrow {}^7F_2$ and the transition $^5D_0 \rightarrow {}^7F_4$ are dominating the spectrum with $I(^5D_0 \rightarrow {}^7F_2)/I(^5D_0 \rightarrow {}^7F_1)$ = 2.10 and $I(^5D_0 \rightarrow {}^7F_4)/I(^5D_0 \rightarrow {}^7F_1)$ = 2.64, respectively (Table 1). The highly forbidden transition $^5D_0 \rightarrow {}^7F_0$ has a quite large intensity (9% of the magnetic dipole transition $^5D_0 \rightarrow {}^7F_1$) indicating that the Eu(III) ion is occupying a site with a C_s, C_n, or C_{nv} symmetry.

Table 1. Integral Intensities of $^5D_0 \rightarrow {}^7F_J$ Transitions Relative to the Magnetic Dipole $^5D_0 \rightarrow {}^7F_1$ in the Emission Spectrum of $[Eu\{DTPA\text{-}ph\text{-}phen\}(H_2O)]^-$ in Aqueous Solutions at Room Temperature

solvent	$\int_{0-0}$	$\int_{0-1}$	$\int_{0-2}$	$\int_{0-3}$	$\int_{0-4}$	$\int_{tot}/\int_{0-1}$
H_2O	0.09	1.00	2.10	0.14	2.64	5.97
D_2O	0.09	1.00	2.11	0.13	2.68	6.01

The luminescence lifetime of the $^5D_0$ level in $[Eu\{DTPA\text{-}ph\text{-}phen\}(H_2O)]^-$ increases from 0.56 to 2.18 ms when going from H_2O to D_2O, reflecting less nonradiative deactivation quenching of the O–D oscillators compared to the O–H oscillators. These data allow to determine the hydration number of the Eu(III) ion in $[Eu\{DTPA\text{-}ph\text{-}phen\}(H_2O)]^-$ using the modified Horrock's equation:[50]

$$q(Eu) = 1.11 \cdot (\Delta k - 0.31 - 0.075 \cdot q^{CONH}) \quad (1)$$

where $\Delta k = 1/\tau_{H_2O} - 1/\tau_{D_2O}$ and q^{CONH} is the number of amide N–H oscillators in the first coordination sphere (here equal to 1). Thus, in $[Eu\{DTPA\text{-}ph\text{-}phen\}(H_2O)]^-$ q was found to be 1.0, so the Eu(III) ion coordinates one water molecule. The overall quantum yield determined under ligand excitation is equal to 2.2% for $[Eu\{DTPA\text{-}ph\text{-}phen\}(H_2O)]^-$ in H_2O solution, and it increases up to 12% in D_2O (Table 2) because of a decreased role of nonradiative transitions for the latter solution as discussed above.

Table 2. Photophysical Parameters of the $[Eu\{DTPA\text{-}ph\text{-}phen\}(H_2O)]^-$ Complex in Aqueous Solutions at Room Temperature[a]

solvent	τ_{obs}/ms	τ_{rad}/ms[b]	Q^{Eu}_{Eu}/%[b]	Q^{L}_{Eu}/%	η_{sens}/%[b]
H_2O	0.56(1)	4.75	12	2.2(2)	19
D_2O	2.18(1)	4.85	45	12(1)	27

[a]Standard deviation (2σ) between parentheses; experimental errors: I_{tot}/I_{MD}, ± 7%; estimated relative errors: n^3, ± 10%; τ_{obs}, ± 2%; Q^{L}_{Ln}, ± 10%; τ_{rad}, ± 12%; Q^{Eu}_{Eu}, ± 12%; η_{sens}, ± 16%. [b]Refractive index for solutions was taken equal to the one of the neat solvents, $n(H_2O)$ = 1.34, $n(D_2O)$ = 1.328; for definition see eqs 2, 3, and 4.

dx.doi.org/10.1021/ic300537y | Inorg. Chem. 2012, 51, 8775–8783

To get an explanation for such a behavior, a comparison between other quantitative characteristics was performed. The sensitization efficiency, η_{sens}, can be calculated according to the formulas:

$$\eta_{sens} = \frac{Q_{Eu}^{L}}{Q_{Eu}^{Eu}} \quad (2)$$

$$Q_{Eu}^{Eu} = \frac{\tau_{obs}}{\tau^{rad}} \quad (3)$$

where Q_{Eu}^{L} and Q_{Eu}^{Eu} are the overall and intrinsic quantum yields, and τ_{obs} and τ_{rad} the observed and radiative lifetimes of Eu(III) $^5D_0$ level. Radiative lifetimes were calculated according to the following formulas:

$$\frac{1}{\tau^{rad}} = A_{MD,0} \cdot n^3 \left(\frac{I_{tot}}{I_{MD}}\right) \quad (4)$$

where $A_{MD,0}$ is the Einstein coefficient and equals 14.65 s^{-1}, n is the refractive index, I_{tot} the total integrated intensity of $^5D_0 \rightarrow {}^7F_J$ (here taken as $J = 0-4$), and I_{MD} the integrated intensity of magnetic-dipole transition $^5D_0 \rightarrow {}^7F_1$.

For the intrinsic quantum yields, values of 12 and 45% were obtained for $[Eu\{DTPA\text{-}ph\text{-}phen\}(H_2O)]^-$ in H_2O and D_2O, respectively, again being in line with the above discussion about the role of nonradiative transitions (Table 2). Although an intrinsic quantum yield of 45% is obtained for the D_2O solution, the estimated sensitization efficiency of the ligand DTPA-ph-phen is quite modest and lies in the range of 19–27%, that in turn results in moderate values of overall quantum yields (Table 2).

Relaxometric Studies. The relaxivity of a Gd(III) complex is defined as the efficiency to enhance the relaxation rate of the neighboring water protons and is expressed in s^{-1} mM^{-1}. It arises from the contributions of short distance interactions between the paramagnetic Gd(III) ion and the coordinated water molecules exchanging with bulk water, the so-called inner sphere interaction (R_1^{is}), and from the long distance interactions related to the diffusion of water molecules near the paramagnetic Gd(III) center, that is, the outer sphere interaction (R_1^{os}). Inner sphere interactions can be described by several parameters,[45,46] such as the number of water molecules coordinated in the first hydration sphere of the complexed ion (q), the electronic relaxation times of Gd(III) (τ_{S1} and τ_{S2}), the rotational correlation time (τ_R), and the residence time of the coordinated water molecules (τ_M).

$$R_1^{p} = R_1^{is} + R_1^{os} \quad (5)$$

$$R_1^{is} = \frac{fq}{T_{1M} + \tau_M} \quad (6)$$

$$\frac{1}{T_{1M}} = \frac{2}{15}\left(\frac{\mu_0}{4\pi}\right)^2 \gamma_H^2 \gamma_S^2 \hbar^2 S(S+1) \frac{1}{r^6}\left[\frac{7\tau_{c2}}{1+(\omega_S\tau_{c2})^2} + \frac{3\tau_{c1}}{1+(\omega_H\tau_{c1})^2}\right] z \quad (7)$$

$$\frac{1}{\tau_{ci}} = \frac{1}{\tau_R} + \frac{1}{\tau_M} + \frac{1}{\tau_{si}} \quad (8)$$

$$\frac{1}{\tau_{S1}} = \frac{1}{5\tau_{S0}}\left[\frac{1}{1+\omega_S{}^2\tau_V{}^2} + \frac{4}{1+4\omega_S{}^2\tau_V{}^2}\right] \quad (9)$$

$$\frac{1}{\tau_{S2}} = \frac{1}{10\tau_{S0}}\left[3 + \frac{5}{1+\omega_S{}^2\tau_V{}^2} + \frac{2}{1+4\omega_S{}^2\tau_V{}^2}\right] \quad (10)$$

where f is the relative concentration of the paramagnetic complex and of the water molecules; γ_S and γ_H are the gyromagnetic ratios of the electron (S) and of the proton (H) respectively; $\omega_{S,H}$ are the Larmor angular frequencies of the electron and of the proton; r is the distance between coordinated water protons and the unpaired electron spin; and $\tau_{c1,2}$ are the correlation times modulating the interaction. These correlation times are defined by eq 8. τ_{S1} and τ_{S2} are field dependent as shown in eqs 9 and 10 where τ_{SO} is the value of $\tau_{s1,2}$ at zero field and τ_v is the correlation time responsible for the modulation of the magnetic interaction.

The outersphere contribution arises from the translational diffusion of water protons around the chelate and can be represented by the Freed model[47] (eqs 11–12).

$$R_1^{os} = \frac{6400\pi}{81}\left(\frac{\mu_0}{4\pi}\right)^2 \gamma_H^2 \gamma_S^2 \hbar^2 S(S+1) NA \frac{[C]}{dD}[7j(\omega_S\tau_D) + 3j(\omega_H\tau_D)] \quad (11)$$

$$j(\omega\tau_D) = \mathrm{Re}\left[\frac{1 + \frac{1}{4}(i\omega\tau_D + \tau_D/\tau_{S1})^{1/2}}{1 + (i\omega\tau_D + \tau_D/\tau_{S1})^{1/2} + \frac{4}{9}(i\omega\tau_D + \tau_D/\tau_{S1}) + \frac{1}{9}(i\omega\tau_D + \tau_D/\tau_{S1})^{3/2}}\right] \quad (12)$$

In these equations, μ_o is the permeability of vacuum ($4\pi \times 10^{-7}$ NA^{-2}), NA is the Avogadro constant (6.02×10^{23} mol^{-1}), $j(\omega\tau_D)$ is the spectral density function described by eq 12, i is the imaginary unit, d is the distance of closest approach, D is the relative molecular diffusion constant, [C] is the molar concentration of paramagnetic ion, and $\tau_D = d^2/D$ is the translational correlation time.

The theoretical fitting of the NMRD profiles takes into account these two contributions to the paramagnetic relaxation rate. Some parameters were fixed during the fitting procedure: the distance (d) of closest approach for the outer sphere contribution was set at 0.36 nm, τ_M was set to 200 ns in good agreement with values reported for other monoamide derivatives of DTPA Gd(III) complexes,[39] the number of coordinated water molecules was set to one ($q = 1$), the relative diffusion constant ($D = 3.0 \times 10^{-9}$ m^2 s^{-1}) and r, the distance between the Gd(III) ion and the proton nuclei of water ($r = 0.31$ nm). The result of the fitting is shown in Figure 4 and Table 3.

The plain line in Figure 4 corresponds to the theoretical fitting of the $[(Gd\{DTPA\text{-}ph\text{-}phen\})_3(H_2O)_3Ru]^-$ data points; the dashed line corresponds to the fitting of the Gd-DTPA data. The NMRD profile of $[(Gd\{DTPA\text{-}ph\text{-}phen\})_3(H_2O)_3Ru]^-$ shows a hump around 20 MHz and

dx.doi.org/10.1021/ic300537y | Inorg. Chem. 2012, 51, 8775–8783

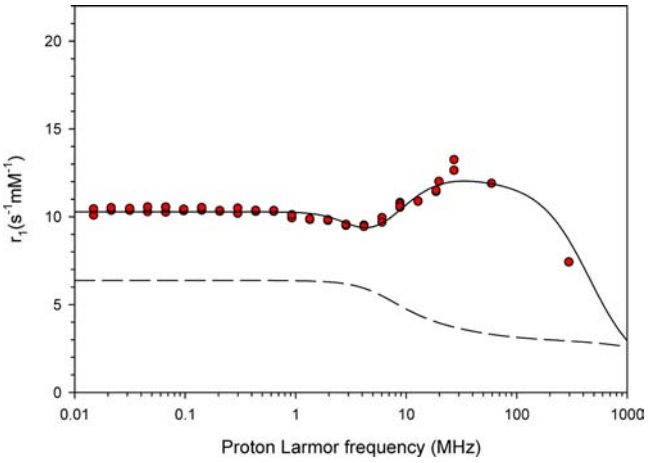

Figure 4. ^{1}H NMRD relaxivity profiles of $[(Gd\{DTPA\text{-}ph\text{-}phen\})_3(H_2O)_3Ru]^-$ (closed circles) and Gd-DTPA (dashed line) in water at 310 K.

Table 3. Parameters Obtained by the Theoretical Fitting of the Proton NMRD Data in Water at 310 K

	$[(Gd\{DTPA\text{-}ph\text{-}phen\})_3(H_2O)_3Ru]^-$	Gd-DTPA[a]
τ_M^{310} [ns]	200[b]	143
τ_R^{310} [ps]	374 ± 5	54 ± 1
τ_{SO}^{310} [ps]	90 ± 1	87 ± 3
τ_V^{310} [ps]	45 ± 1	25 ± 3
r_1 [s^{-1} mM^{-1}] at 20 MHz	12.0	3.8

[a]From ref 51. [b]Fixed value.

follows the profile of a high molecular weight complex. The τ_{SO} value at 310 K can be considered similar to the value of the Gd-DTPA complex. The tumbling rate of $[(Gd\{DTPA\text{-}ph\text{-}phen\})_3(H_2O)_3Ru]^-$ agrees with the size of the complex and is, as expected, slower than the tumbling rate of Gd-DTPA. In addition, this value shows the absence of local mobility of the Gd-DTPA moieties. This results in an increased relaxivity of 12.0 s^{-1} mM^{-1} per Gd(III) ion and 36.0 s^{-1} mM^{-1} per metallostar complex at 20 MHz and 310 K.

Compared to other metallostars,[7,19] such as for example $\{Ru[Gd_2bpy(DTTA)_2(H_2O)_4]_3\}^{4-}$ $\{Fe[Gd_2bpy\text{-}(DTTA)_2(H_2O)_4]_3\}^{4-}$, the metallostar reported in this study has a lower relaxivity at 20 MHz and 37 °C ($r_1 \sim 25$ s^{-1} mM^{-1} for $\{Ru[Gd_2bpy(DTTA)_2(H_2O)_4]_3\}^{4-}$ and $r_1 \sim 18$ s^{-1} mM^{-1} for $\{Fe[Gd_2bpy(DTTA)_2(H_2O)_4]_3\}^{4-}$). This difference is mainly due to the lower number of coordinated water molecules ($q = 1$ for our compound and $q = 2$ for $\{Ru[Gd_2bpy(DTTA)_2(H_2O)_4]_3\}^{4-}$ and $\{Fe[Gd_2bpy\text{-}(DTTA)_2(H_2O)_4]_3\}^{4-}$), resulting in lower relaxation.

$[(Gd\{DTPA\text{-}ph\text{-}phen\})_3(H_2O)_3Ru]^-$ was also subjected to a relaxometric study determining the interaction of the complex with human serum albumin (HSA). HSA is an important protein in the plasma of the human body (concentration of 4–4.5%) and 1,10-phenanthroline is known to interact with HSA.[40] Interaction of the Gd(III) complex with HSA should result in increased paramagnetic relaxation rates because of an increased rotational correlation time. The change of the observed relaxation rate depends on the intensity of the magnetic field, on the proportion of bound contrast agents and, therefore, on the strength of the interaction. Figure 5 shows the proton NMRD profile of $[(Gd\{DTPA\text{-}ph\text{-}phen\})_3(H_2O)_3Ru]^-$

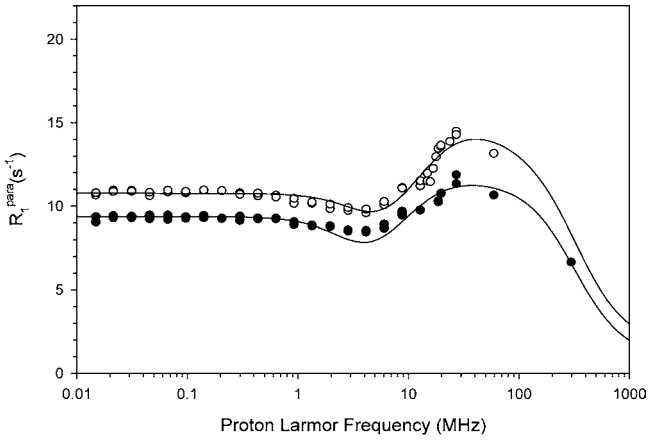

Figure 5. Proton paramagnetic relaxation rate of solutions of $[(Gd\{DTPA\text{-}ph\text{-}phen\})_3(H_2O)_3Ru]^-$ (0.896 mM) in water (closed circles) and in aqueous solution of HSA 4% (open circles). Both lines through the data are drawn to guide the readers' eyes.

in water and in an aqueous solution of 4% HSA. The slight increase of paramagnetic relaxation in the presence of HSA can be explained by a viscosity increase induced by HSA (0.87 mPa·s with HSA compared to 0.69 mPa·s without HSA at 310 K) resulting in an increased value of τ_R and a decreased value of the relative diffusion constant D.

Analysis of the paramagnetic proton relaxation rate of the complex in solution containing 4% of HSA and increasing the amounts of $[(Gd\{DTPA\text{-}ph\text{-}phen\})_3(H_2O)_3Ru]^-$ confirms that the presence of HSA does not induce significant modifications (Figure 6). The slight increase in paramagnetic relaxation over

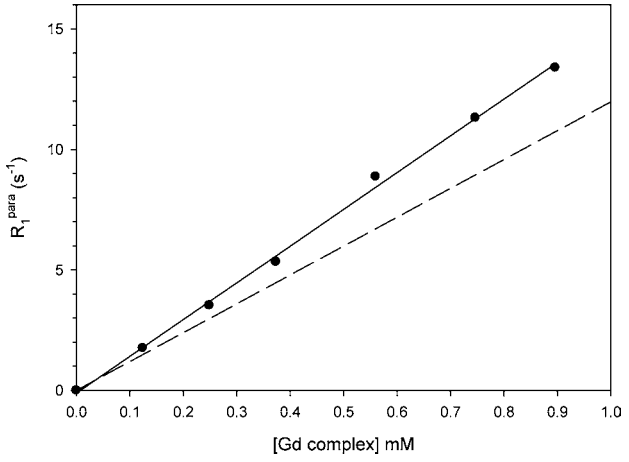

Figure 6. Proton paramagnetic relaxation rate of $[(Gd\{DTPA\text{-}ph\text{-}phen\})_3(H_2O)_3Ru]^-$ in an aqueous solution of 4% HSA at 20 MHz and 310 K. The dashed line represents the data obtained in water.

the investigated concentration range indicates a negligible interaction between $[(Gd\{DTPA\text{-}ph\text{-}phen\})_3(H_2O)_3Ru]^-$ and HSA, rendering any estimation of K_a and r_C^1 difficult.

CONCLUSION

This paper presents the design of a new Gd(III)–Ru(II) based metallostar complex, $[(Gd\{DTPA\text{-}ph\text{-}phen\})_3(H_2O)_3Ru]^-$. The complex exhibits red broad-band luminescence centered at 610 nm under excitation at 450 nm with a quantum yield of 4.8%. The increase in molecular volume of $[(Gd\{DTPA\text{-}ph\text{-}phen\})_3(H_2O)_3Ru]^-$ results in a decrease of the tumbling rate

dx.doi.org/10.1021/ic300537y | Inorg. Chem. 2012, 51, 8775–8783

by a factor of 6.9 compared to Gd-DTPA (Magnevist). ^{1}H NMRD measurements of $[(Gd\{DTPA\text{-}ph\text{-}phen\})_3(H_2O)_3Ru]^-$ in turn show an enhanced r_1 relaxivity value up to 12.0 s^{-1} mM^{-1} per Gd(III) ion corresponding to 36.0 s^{-1} mM^{-1} per metallostar complex at 20 MHz and 310 K. Taking into account both favorable luminescence and relaxometric properties, $[(Gd\{DTPA\text{-}ph\text{-}phen\})_3(H_2O)_3Ru]^-$ can be further explored as probe for MRI and luminescence-based imaging.

■ ASSOCIATED CONTENT

Supporting Information

^{1}H (Figure S1) and 2D COSY (Figure S2) NMR spectra of ligand DTPA-ph-phen, absorption spectra of the ligand, $[Gd\{DTPA\text{-}ph\text{-}phen\}(H_2O)]^-$ and $[(Gd\{DTPA\text{-}ph\text{-}phen\})_3(H_2O)_3Ru]^-$complexes (Figure S3). ^{1}H NMR spectrum of $[(La\{DTPA\text{-}ph\text{-}phen\})_3(H_2O)_3Ru]^-$complex. This material is available free of charge via the Internet at http://pubs.acs.org.

■ AUTHOR INFORMATION

Corresponding Author

*E-mail: tatjana.vogt@chem.kuleuven.be.

Notes

The authors declare no competing financial interest.

■ ACKNOWLEDGMENTS

G.D., P.V., T.N.P.-V., and K.B. acknowledge the IWT Flanders (Belgium) and the FWO-Flanders (project G.0412.09) for financial support. S.V.E. is a visiting postdoctoral fellow of the FWO-Flanders (project G.0412.09). S.L., L.V.E., and R.N.M. thank the ARC (program of Research of the French Community of Belgium, research contract 00/05-258, 05/10-335 and AUWB-2010—10/15-UMONS-5), FNRS, ENCITE, the framework of COST D38 (Metal-Based Systems for Molecular Imaging Applications) and TD1004 (Theragnostics), the European Network of Excellence EMIL (European Molecular Imaging Laboratories) program LSCH-2004-503569 and the Center for Microscopy and Molecular Imaging (CMMI, supported by the European Regional Development Fund and the Walloon Region) for their support. ESI-MS measurements were made by Mr. Dirk Henot and Mr. Bert Demarsin, and ICP-MS measurements were performed by Michèle Vanroelen (Department of Chemical Engineering). Mr. Karel Duerinckx is acknowledged for his help in the NMR measurements. We also thank Mr. Servaas Michielssens for his development of the framework molecular model.

■ REFERENCES

(1) Caravan, P.; Ellison, J. J.; McMurry, T. J.; Lauffer, R. B. *Chem. Rev.* **1999**, *99*, 2293.
(2) Merbach, A. E.; Toth, E. *The chemistry of contrast agents in medical magnetic resonance imaging*; John Wiley & Sons, Ltd: New York, 2001.
(3) Bonnet, C. S.; Toth, E. *C. R. Chim.* **2010**, *13*, 700.
(4) Frullano, L.; Meade, T. J. *J. Biol. Inorg. Chem.* **2007**, *12*, 939.
(5) Louie, A. Y. *Chem. Rev.* **2010**, *110*, 3146.
(6) Bernhard, C.; Goze, C.; Rousselin, Y.; Denat, F. *Chem. Commun.* **2010**, *46*, 8267.
(7) Moriggi, L.; Aebischer, A.; Cannizzo, C.; Sour, A.; Borel, A.; Bunzli, J. C. G.; Helm, L. *Dalton Trans.* **2009**, 2088.
(8) Caravan, P. *Chem. Soc. Rev.* **2006**, *35*, 512.
(9) Kowalewski, J.; Nordenskiold, L.; Benetis, N.; Westlund, P. O. *Prog. Nucl. Magn. Reson. Spectrosc.* **1985**, *17*, 141.
(10) Parac-Vogt, T. N.; Kimpe, K.; Laurent, S.; Pierart, C.; Vander Elst, L.; Muller, R. N.; Binnemans, K. *Eur. Biophys. J.* **2006**, *35*, 136.
(11) Parac-Vogt, T. N.; Kimpe, K.; Laurent, S.; Pierart, C.; Vander Elst, L.; Muller, R. N.; Binnemans, K. *Eur. J. Inorg. Chem.* **2004**, 3538.
(12) Anelli, P. L.; Lattuada, L.; Lorusso, V.; Schneider, M.; Tournier, H.; Uggeri, F. *Magn. Reson. Mater. Phys.* **2001**, *12*, 114.
(13) Grist, T. M.; Korosec, F. R.; Peters, D. C.; Witte, S.; Walovitch, R. C.; Dolan, R. P.; Bridson, W. E.; Yucel, E. K.; Mistretta, C. A. *Radiology* **1998**, *207*, 539.
(14) Lauffer, R. B.; Parmelee, D. J.; Ouellet, H. S.; Dolan, R. P.; Sajiki, H.; Scott, D. M.; Bernard, P. J.; Buchanan, E. M.; Ong, K. Y.; Tyeklar, Z.; Midelfort, K. S.; McMurry, T. J.; Walovitch, R. C. *Acad. Radiol.* **1996**, *3*, S356−S358.
(15) Caravan, P.; Cloutier, N. J.; Greenfield, M. T.; McDermid, S. A.; Dunham, S. U.; Bulte, J. W. M.; Amedio, J. C.; Looby, R. J.; Supkowski, R. M.; Horrocks, W. D.; McMurry, T. J.; Lauffer, R. B. *J. Am. Chem. Soc.* **2002**, *124*, 3152.
(16) Comblin, V.; Gilsoul, D.; Hermann, M.; Humblet, V.; Jacques, V.; Mesbahi, M.; Sauvage, C.; Desreux, J. F. *Coord. Chem. Rev.* **1999**, *185*−*6*, 451.
(17) Jacques, V.; Desreux, J. F. *Top. Curr. Chem.* **2002**, *221*, 123.
(18) Livramento, J. B.; Toth, E.; Sour, A.; Borel, A.; Merbach, A. E.; Ruloff, R. *Angew. Chem., Int. Ed.* **2005**, *44*, 1480.
(19) Livramento, J. B.; Sour, A.; Borel, A.; Merbach, A. E.; Toth, V. *Chem.—Eur. J.* **2006**, *12*, 989.
(20) Aime, S.; Barge, A.; Cabella, C.; Crich, S. G.; Gianolio, E. *Curr. Pharm. Biotechnol.* **2004**, *5*, 509.
(21) Beeby, A.; Botchway, S. W.; Clarkson, I. M.; Faulkner, S.; Parker, A. W.; Parker, D.; Williams, J. A. G. *J. Photochem. Photobiol. B* **2000**, *57*, 83.
(22) Koullourou, T.; Natrajan, L. S.; Bhavsar, H.; Pope, S. J. A.; Feng, J.; Narvainen, J.; Shaw, R.; Scales, E.; Kauppinen, R.; Kenwright, A. M.; Faulkner, S. *J. Am. Chem. Soc.* **2008**, *130*, 2178.
(23) Kotkova, Z.; Kotek, J.; Jirak, D.; Jendelova, P.; Herynek, V.; Berkova, Z.; Hermann, P.; Lukes, I. *Chem.—Eur. J.* **2010**, *16*, 10094.
(24) Huber, M. M.; Staubli, A. B.; Kustedjo, K.; Gray, M. H. B.; Shih, J.; Fraser, S. E.; Jacobs, R. E.; Meade, T. J. *Bioconjugate Chem.* **1998**, *9*, 242.
(25) Jennings, L. E.; Long, N. J. *Chem. Commun.* **2009**, 3511.
(26) Tu, C.; Ma, X.; House, A.; Kauzlarich, S. M.; Louie, A. Y. *J. Am. Chem. Soc.* **2010**, *132*, 2016.
(27) Mulder, W.J. M.; Koole, R.; Brandwijk, R. J.; Storm, G.; Chin, P. T. K.; Strijkers, G. J.; de Mello Donegá, C.; Nicolay, K.; Griffioen, A. W. *Nano Lett.* **2006**, *6*, 1.
(28) Stasiuk, G. J.; Tamang, S.; Imbert, D.; Poillot, C.; Giardiello, M.; Tisseyre, C.; Barbier, E. L.; Fries, P. H.; de Waard, M.; Reiss, P.; Mazzanti, M. *ACS Nano* **2011**, 8193.
(29) Charbonniere, L. J.; Ziessel, R.; Montalti, M.; Prodi, L.; Zaccheroni, N.; Boehme, C.; Wipff, G. *J. Am. Chem. Soc.* **2002**, *124*, 7779.
(30) Fernandez-Moreira, V.; Thorp-Greenwood, F. L.; Coogan, M. P. *Chem. Commun.* **2010**, *46*, 186.
(31) Kalyanasundaram, K. *Coord. Chem. Rev.* **1982**, *46*, 159.
(32) Juris, A.; Balzani, V.; Barigelletti, F.; Campagna, S.; Belser, P.; Vonzelewsky, A. *Coord. Chem. Rev.* **1988**, *84*, 85.
(33) Lo, K. K. W.; Lee, T. K. M.; Lau, J. S. Y.; Poon, W. L.; Cheng, S. H. *Inorg. Chem.* **2008**, *47*, 200.
(34) Anderson, A. J.; Jayanetti, S.; Mayanovic, R. A.; Bassett, W. A.; Chou, I. M. *Am. Mineral.* **2002**, *87*, 262.
(35) Lazarides, T.; Sykes, D.; Faulkner, S.; Barbieri, A.; Ward, M. D. *Chem.—Eur. J.* **2008**, *14*, 9389.
(36) Baca, S. G.; Adams, H.; Sykes, D.; Faulkner, S.; Ward, M. D. *Dalton Trans.* **2007**, 2419.
(37) Senechal-David, K.; Pope, S. J. A.; Quinn, S.; Faulkner, S.; Gunnlaugsson, T. *Inorg. Chem.* **2006**, *45*, 10040.
(38) Nonat, A. M.; Allain, C.; Faulkner, S.; Gunnlaugsson, T. *Inorg. Chem.* **2010**, *49*, 8449.

(39) Dehaen, G.; Eliseeva, S. V.; Kimpe, K.; Laurent, S.; Vander Elst, L.; Muller, R. N.; Dehaen, W.; Binnemans, K.; Parac-Vogt, T. N. *Chem.—Eur. J.* **2012**, *18*, 293.
(40) Dehaen, G.; Verwilst, P.; Eliseeva, S. V.; Laurent, S.; Vander Elst, L.; Muller, R. N.; De Borggraeve, W. M.; Binnemans, K.; Parac-Vogt, T. N. *Inorg. Chem.* **2011**, *50*, 10005.
(41) Girardot, C.; Lemercier, G.; Mulatier, J. C.; Chauvin, J.; Baldeck, P. L.; Andraud, C. *Dalton Trans.* **2007**, 3421.
(42) Eaton, D. F. *Pure Appl. Chem.* **1988**, *60*, 1107.
(43) *Avogadro: an open-source molecular builder and visualization tool*, Version 1.0.0; 2011; http://avogadro.openmolecules.net/.
(44) Rappe, A. K.; Casewit, C. J.; Colwell, K. S.; Goddard, W. A.; Skiff, W. M. *J. Am. Chem. Soc.* **1992**, *114*, 10024.
(45) Muller, R. N., Declercq, D., Vallet, P., Giberto, F., Daminet, B., Fischer, H. W., Maton, F., Van Haverbeke, Y. In *Proceedings of the ESMRMB, 7th Annual Congress*, May 2−5, Strasbourg, France, 1990.
(46) Solomon, I. *Phys. Rev.* **1955**, *99*, 559.
(47) Bloembergen, N. *J. Chem. Phys.* **1957**, *27*, 572.
(48) Freed, J. H. *J. Chem. Phys.* **1978**, *68*, 4034.
(49) Onishi, H.; Sekine, K. *Talanta* **1972**, *19*, 473.
(50) Supkowski, R. M.; Horrocks, W. D. *Inorg. Chim. Acta* **2002**, *340*, 44.
(51) Laurent, S.; Vander Elst, L.; V.; Botteman, F.; Muller, R. N. *Eur. J. Inorg. Chem.* **2008**, 4369.